JOC The Journal of Organic Chemistry

Article

pubs.acs.org/joc

Synthesis, Structure, and Bonding of 1-Oxa-6,6aλ^4-chalcogenopentalenes and Related Derivatives; The Role of Intramolecular Coordination

Poonam Rajesh Prasad,[†] Karuthapandi Selvakumar,[†] Harkesh B. Singh,*[,†] and Ray J. Butcher[‡]

[†]Department of Chemistry, Indian Institute of Technology Bombay, Powai, Mumbai 400076, India

[‡]Department of Chemistry, Howard University, Washington, DC 20059, United States

Supporting Information

ABSTRACT: The synthesis and characterization of a series of alicyclic organochalcogen compounds derived from 2-chloro-1-formyl-3-hydroxymethylenecyclohexene (**16**) are described. The reaction of **16** with disodium disulfide afforded an unexpected 1-oxa-6,6aλ^4-dithiapentalene **33**, whereas the reaction of disodium diselenide afforded 1-oxa-6,6aλ^4-diselenapentalene **34**, along with 1,6-dioxa-6a-selenapentalene **35**. In contrast, when **16** was treated with Na_2Te_2, it resulted in the formation of 1-oxa-6,6aλ^4-ditellurapentalene **36** along with 1,6-dioxa-6a-tellurapentalene **37** and cyclic monotelluride **38**. The oxidation of 1-oxa-6,6aλ^4-diselenapentalene **34** with *m*-CPBA provided the corresponding 1-oxa-6,6aλ^4-diselenapentalene-6,6aλ^4-dioxide **39** in which both of the selenium atoms were found to be oxidized. The 1-oxa-6,6aλ^4-dichalcogenopentalenes **33**, **34**, and **36** are stabilized by 3c-4e bond resulting from intramolecular E···O interaction. The donor oxygen donates a lone pair of electrons to the σ^* orbital of acceptor E−E bond (E = S, Se, and Te) whose σ bond already has its bond pair electrons. The existence of intramolecular E···O interactions was established by multinuclear NMR spectroscopy, single crystal X-ray analysis, and computational studies. The single crystal X-ray structures of compounds **33**, **34**, and **36** reveal that the molecules are almost planar. Nucleus-independent chemical shifts were calculated to compare the aromaticity in both the five-membered rings of **33**, **34**, **36** and 1,6-dioxa-6a-chalcopentalenes (**35** and **37**). The isotropic shift values of the covalently fused five-membered heterocyclic rings are more negative than the five-membered heterocyclic rings formed by intramolecular coordination.

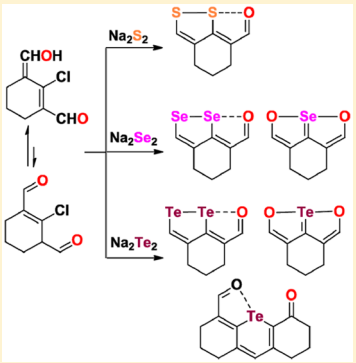

INTRODUCTION

The chemistry of arylchalcogen derivatives having intramolecular E···X (E = Se, Te; X = N, O, S) secondary bonding interaction (SBI) has attracted considerable current interest owing to their use in various fields such as (a) stabilization and isolation of unstable organochalcogen compounds,[1−5] (b) as reagents in organic synthesis,[6−10] (c) precursors for nanomaterials,[11,12] and (d) selenoenzyme mimics.[5,13−15] In addition to these, the intramolecular interactions are also responsible for the specific redox activity of organochalcogen compounds.[16] Recently, much attention has been devoted to the arylchalcogen derivatives having two ortho coordinating groups because of their contrasting reactivity and stability compared to the analogous compounds with one ortho coordinating group. For example, the attempted synthesis of respective oxides of 2,6-bis[(dimethylamino)methyl]phenyl methyl selenide and telluride, having two intramolecularly coordinating amino groups, resulted in the isolation of novel selenenium **1** and tellurenium **2** cations, respectively (Chart 1).[1] Kersting et al. and Zade et al. reported that the attempted synthesis of *N*,*N*-dialkyl/diphenylisophthalamides and *N*,*N*-dialkyl/diphenyl-2-bromo-5-*tert*-butylisophthalamides dichalcogenides having two amide groups always led to the formation of cyclized ebselen derivatives **3a**−**4b** and the corresponding sulfur and tellurium analogues **5a**−**6b**.[17−19] Similar observations were also reported by Mugesh and co-workers[20] where the attempted synthesis of bis(*N*,*N*-dimethyl 2,6-oxazoline)-2-phenyl diselenide resulted in the isolation of ebselen analogue **7** via intramolecular cyclization. However, the analogous diselenides with one coordinating group at ortho position are quite stable. Attempts to synthesize 4-*tert*-butyl-2,6-di(formyl)phenylselenenyl bromide from the reaction of bis(2,6-diformyl-4-*tert*-butylphenyl)diselenide[21] with bromine resulted in the formation of novel cyclic selenenate ester **8**. Similarly Selvakumar et al.[22] and Singh et al.[23] demonstrated the isolation of novel selenenate esters **9a**−**9b** and **10a**−**10c**, respectively. Parnham et al.[24] isolated the ebselen analogues **11** owing to the presence of two coordinating groups. Back and co-workers and Singh and co-workers have isolated the bicyclic selenuranes **12**[25] and **13a**,[26] respectively, via oxidation reaction of selenides containing two hydroxyl or carboxyl groups, while bicyclic tellurane **13b** was isolated from the oxidation reaction of telluride having two ester groups.[27] Recently, Selvakumar et al. isolated the tellurenate ester **14**,[27] which was stabilized by strong intramolecular coordination.

Received: January 26, 2016
Published: March 24, 2016

DOI: 10.1021/acs.joc.6b00173
J. Org. Chem. 2016, 81, 3214−3226

Chart 1. 2,6-Disubstituted Aryl-Based Selenium Derivatives

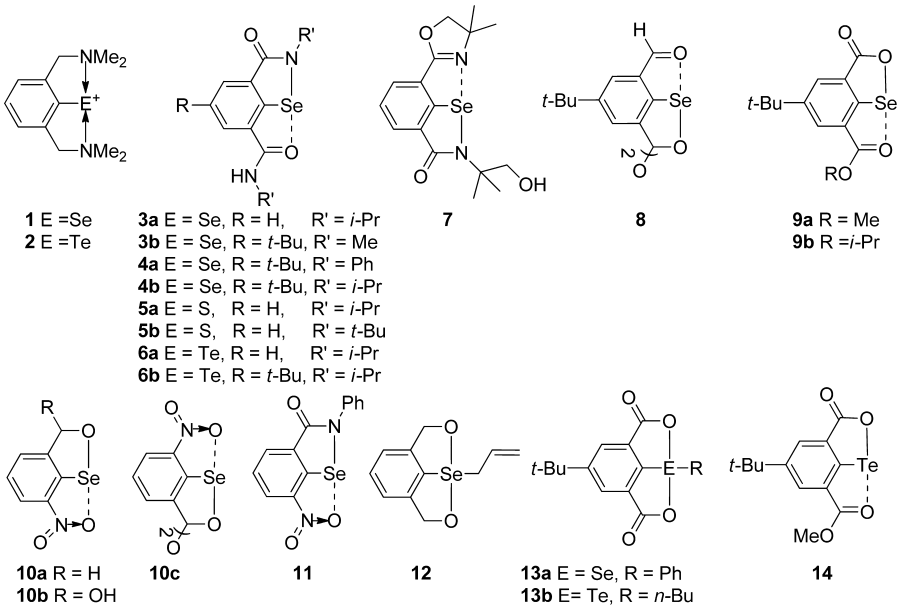

The theoretical studies on facile cyclization of diaryl diselenides/aryl selenenyl halides revealed that both the presence of additional coordinating group (steric crowding) and strong intramolecular interaction introduce a distortion in the planarity of the aromatic ring which leads to facile intramolecular cyclization and in no case the desired diselenide could be isolated.[22]

In view of the novel reactivity of the diaryl dichalcogenide/aryl chalcogenyl halides and related derivatives having two groups R and R′ (where R and R′ = CHO, COOH, COOMe, COONHR, CH_2OH, and NO_2) derived from aryl bromide (e.g., **15**, Chart 2), with Na_2E_2 (E = Se, Te), we decided to explore the reactivity of the analogous alicyclic precursor with Na_2E_2 (E = S, Se, Te). The precursor 2-chloro-1-formyl-3-hydroxymethylenecyclohexene (**16**) exists in two resonance structures, i.e., enol form (**16**) and keto form (**16′**). The enol form is expected to be more predominant in solution state rather than the keto form due to the resonance stabilization in the former. These types of skeletons are commonly used in the synthesis of organic dyes and polymer chemistry.[28]

Chart 2. Disubstituted Aryl and Alicyclic-Based Precursors

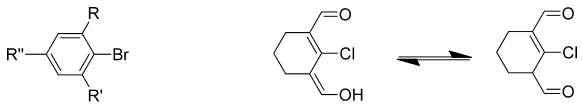

Interestingly, the reactions of 2-chloro-1-formyl-3-hydroxymethylenecyclohexene (**16**) with disodium dichalcogenides afforded new classes of unexpected 1-oxa-6,6aλ^4-dichalcogenopentalenes and 1,6-dioxa-6a-chalcogenopentalenes, where three chalcogen atoms were bonded in a linear fashion (*vide infra*). Such types of unsymmetrical 1-oxa-6,6aλ^4-dichalcogenopentalenes stabilized by intramolecular interaction are not well studied. Only a few examples are reported with sulfur.[29,30] For instance, 1,6-dioxa-6a-chalcogenopentalenes have been prepared by using different synthetic strategies (Chart 3). 1,6,6aλ^4-Trithiapentalene (**17**)[31] was one of the first examples having two fused thiapentalene rings. This has been studied extensively for the planarity of the fused five-membered heterocyclic rings and unique C_2v-symmetric structure at the tricoordinate central sulfur atom.[32−34] Subsequently, related structures and their aza analogues were reported (**18**−**29**).[35−41] 1,6-Dioxa-6aλ^4-thia[42] (**25**−**26**) and selenapentalene[39] (**27**−**28**) were prepared by the reaction of pyran-4-thiones and pyran-4-selones, respectively, in the presence of thallium trifluorate. Later, Detty et al.[43] reported the synthesis of the first tellurium analogue, 2,5-diphenyl-1,6-dioxa-6aλ^4-tellurapentalene (**29**) by the reaction of 3-methyl-5-phenyl-l,2-oxatellurol-ium chloride with benzyl chloride. This class of compounds is interesting in terms of their structure and bonding and is used as sensitizers in electrographic compositions. These are also used as molecular electron donors and charge emitters in multilayer photoconductive elements.[44]

Herein, we describe a new methodology for the synthesis of intramolecularly stabilized 1-oxa-6,6aλ^4-dichalcogenopentalenes

Chart 3. 1,6-Dioxa-6aλ^4- chalcopentalene Derivatives

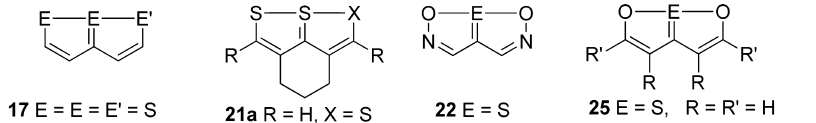

DOI: 10.1021/acs.joc.6b00173
J. Org. Chem. 2016, 81, 3214−3226

Scheme 1. Reaction of Na_2S_2 with 16[a]

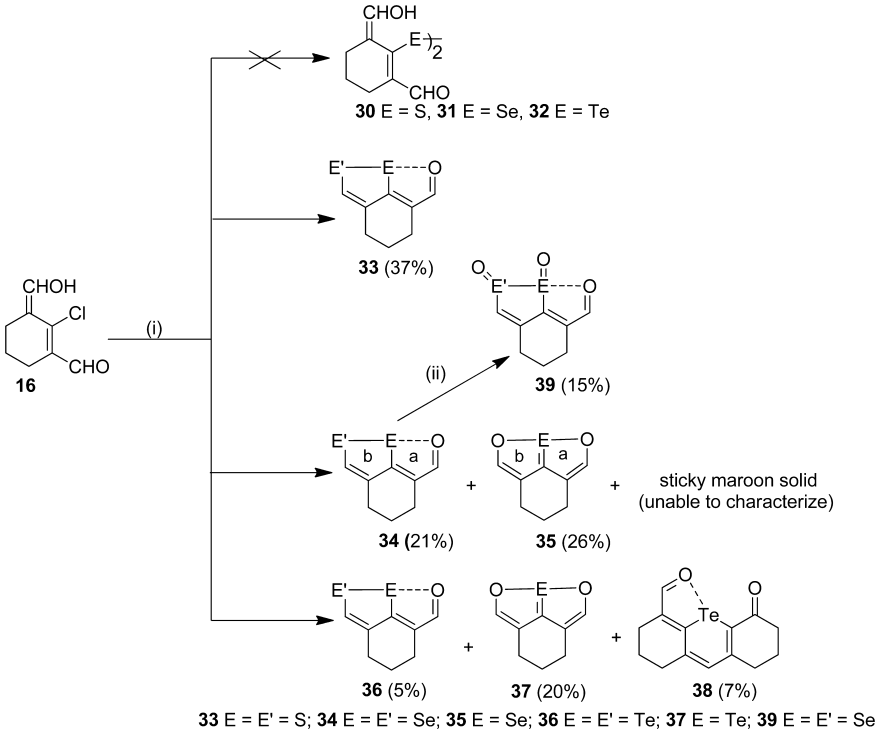

[a]Reagents and conditions: (i) Na_2E_2 (E = S, Se, Te), THF, HMPA, reflux, 6 h; (ii) *m*-CPBA, dry CH_2Cl_2, −78 °C.

Scheme 2. Plausible Mechanism for the Formation of 1-Oxa-6,6aλ^4-dichalcogenopentalenes (33, 34 and 36) and 1,6-Dioxa-6a-chalcogenopentalenes (35 and 37)

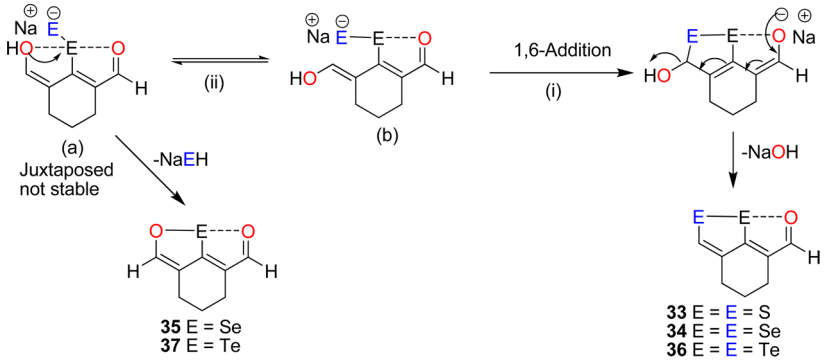

and related derivatives in one-pot synthesis and describe their structure and bonding.

RESULTS AND DISCUSSION

Synthesis. The precursor, 2-chloro-1-formyl-3-hydroxymethylenecyclohexene (**16**), was prepared by the reaction of cyclohexanone with phosphorus oxychloride and dimethylformamide by following the literature procedure[45] with slight modification in the aqueous workup. Compound **16** is not stable even at low temperature and decomposes rapidly within 2 days at room temperature and must be handled with care. Therefore, the reactions were carried out with freshly prepared **16** to give good yields of the products. Attempted synthesis of desired diorganodichalcogenides **30**−**32** by the reaction of **16** with disodium dichalcogenides (Na_2E_2; E = S, Se, Te) under reflux condition led to the formation of unexpected 1-oxa-6,6aλ^4-dichalcogenopentalenes **33**, **34**, **36** and 1,6-dioxa-6a-chacogenopentalenes **35** and **37**. The reaction of Na_2S_2 with **16** afforded 1-oxa-6,6aλ^4-dithiapentalene **33** (Scheme 1). The compounds were purified by column chromatography using petroleum ether and ethyl acetate (2−10%) as eluent.

In the reaction of disodium diselenide, the first fraction isolated was 1-oxa-6,6aλ^4-diselenapentalene **34** as an orange solid. The second fraction was 1,6-dioxa-6a-selenapentalene **35** as a yellow colored solid, and the third fraction was as a maroon sticky colored solid (could not be characterized). The fourth fraction was the unreacted starting material **16**. Similarly, in the case of the Na_2Te_2 reaction, four fractions were obtained. The first fraction isolated was 1-oxa-6,6aλ^4-ditellurapentalene **36** as a red colored solid, and the second fraction was 1,6-dioxa-6a-tellurapentalene **37** as a yellowish orange colored solid. The third fraction was cyclic monotelluride **38** as a dark red solid, and fourth one was the unreacted starting material **16**. The yield of the 1-oxa-6,6aλ^4-ditellurapentalene **36** is quite low in comparison to 1-oxa-6,6aλ^4-dithaentalene **33** and 1-oxa-6,6aλ^4-diselenapentalene **34**.

DOI: 10.1021/acs.joc.6b00173
J. Org. Chem. 2016, 81, 3214−3226

A quick understanding of the formation of 1-oxa-6,6aλ^4-dichalcogenopentalenes and the 1,6-dioxa-6a-chalcogenopentalenes could be reached by invoking the nature of juxtaposed chalcogen−chalcogen interactions. In general, when the divalent central chalcogen encounters more than one peripheral chalcogens, the nonbonded interaction becomes repulsive.[1,46] As a result, the entire system tries to readjust to stabilize itself via either conformational rearrangement or undergoing further reaction to form more stable products. This results in the decomposition of the intermediate to form 1,6-dioxa-6a-chalcogenopentalene (**35** and **37**) via the nucleophilic attack of hydroxyl function on the central electrophilic chalcogen (*vide infra*), or it undergoes 1,6-addition followed by elimination to afford the unsymmetrical 1-oxa-6,6aλ^4-dichalcogenopentalenes (**33**, **34**, and **36**) via the following mechanisms (Scheme 2) .

Singh and co-workers have reported a similar mechanism for the formation of selenenate/tellurenate esters via intramolecular cyclization.[22] However, the mechanism involving the formation of cyclic monotelluride **38** is not clear. Oxidation of **34** with *m*-CPBA at −78 °C gave 1-oxa-6,6aλ^4-diselenapentalene-6,6aλ^4-dioxide **39** as a brown solid. In comparison to **34**, 1-oxa-6,6aλ^4-diselenapentalene-6,6aλ^4-dioxide **39** was found to be unstable at ambient temperature. Product **39** decomposed slowly and led to the formation of 1-oxa-6,6aλ^4-diselenapentalene **34** even at −13 °C. Kice and Reich and their co-workers have reported a similar observation for five-membered 4,4-dimethyl-1,2-diselenolane-1-oxide,[47,48] which was found to be unstable and decomposed even at −20 °C. To our knowledge, 1-oxa-6,6aλ^4-diselenapentalene-6,6aλ^4-dioxide **39** is the first example in which both of the adjacent selenium(IV) atoms are part of the five-membered heterocyclic ring. It is important to emphasize here that compound **39** is expected to be a mixture of diastereomers, similar to the chiral behavior of selenoxides.[49] However, the observation of clean ^{1}H, ^{13}C, and ^{77}Se NMR spectra suggests (Supporting Information) that compound **39** does not exist as a mixtures of diastereomers. This could be due to the prevalence of its achiral hydrated form, −C−Se(OH)$_2$−Se(OH)$_2$−C−, in solution due to the inherent hygroscopic behavior of selenoxides.[49] Alternately, the possibility of its structural isomer **39a** cannot be ruled out. To compare the structural features of tellurium systems (**35** and **36**) with related aromatic derivatives, compound **40** was synthesized following the procedure suggested in the literature.[27] The newly synthesized derivatives were fully characterized by elemental analysis, common spectroscopic tools (^{1}H, ^{13}C, ^{77}Se, and ^{125}Te NMR and FT-IR spectroscopy) and mass spectrometry (*vide infra*). The structures of compounds **33**−**38** were further corroborated by single crystal X-ray crystallography (*vide infra*).

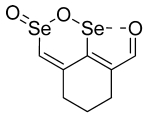

39a

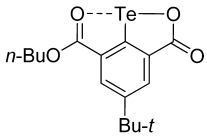

40

Spectral Features of 1-Oxa-6,6aλ^4-dichalcogenopentalenes and 1,6-Dioxa-6a-chalcopentalenes. In the ^{1}H NMR spectra of 1-oxa-6,6aλ^4-dichalcogenopentalenes **33**, **34**, and **36**, the vinyl protons appeared at 7.50, 8.37, and 9.88 ppm, respectively, and the formyl protons appeared at 9.33, 9.45, and 9.97 ppm, respectively. The vinyl proton signals and formyl protons are significantly downfield and upfield shifted, respectively, than the corresponding proton signals in the starting material (7.26 and 10.16 ppm). That indicates the delocalization of electron density in the cyclic systems. Interestingly, in 1,6-dioxa-6a-selenapentalene **35**, the vinylic and the formyl proton signals merge to give an average signal at 8.70 ppm. This implies that the protons have more resemblance to the vinylic proton than the formyl proton. It happens with tellurapentalene **37** as well, and the corresponding protons appear at 9.02 ppm. This indicates that both the oxygen atoms are covalently bonded to selenium/tellurium atoms leading to symmetrical structures that were further corroborated with X-ray crystallographic and computational studies. In the case of monotelluride **38**, the vinyl protons appeared at 6.69 ppm and the formyl proton at 9.95 ppm, which are significantly downfield as compared to the 1-oxa-6,6aλ^4-ditellurapentalene **36** (9.88 ppm). In the ^{1}H NMR spectrum of compound **39**, the formyl proton appears at 9.70 ppm, which is significantly downfield as compared to the corresponding 1-oxa-6,6aλ^4-diselenapentalene **34**. In the cases of **33**, **34**, and **36**, the formyl carbons appeared at 182.5, 181.3, and 179.7 ppm, respectively, which suggests that the formyl carbons are shifted to the upfield region in going from S to Te. Compounds **35** and **37** show five sets of peaks (C2═C6, C3═C5, C7═C8) which further indicate that the molecules are symmetrical, and the formyl carbons are absent (Figure S12). In the case of **38**, two peaks appeared at 200.3 and 188.4 ppm corresponding to the formyl carbon and the ketone carbonyl carbon, respectively.

The ^{77}Se NMR spectrum of **34** showed two signals, one at 884 ppm and another broad one at 502.58 ppm, which could be resolved into two signals at 502.37 and 502.79 ppm with a coupling constant of 40 Hz (^2J Se−H) (Figure S7). The broad peak chemical shift (502.58 ppm) is downfield in comparison to the chemical shift observed for related diselenide, bis(2,6-diformyl-4-*tert*-butylphenyl)diselenide (458 ppm),[21] but close to that observed for tetramethyl-2,2′-diselanediylbis(5-(*tert*-butyl)isophthalate) (519 ppm).[22] The chemical shift at 884 ppm is closer to the chemical shift values observed for the selenium atoms in selenazole like heterocycles,[19,20] where the arylselenium moiety is directly bonded to a nitrogen atom. The diaryl selenoxide derivatives also have similar chemical shifts.[50] Therefore, the signal at 884 ppm must be associated with the selenium (central) which is coordinated to oxygen. The split peaks at ∼503 ppm are associated with the peripheral selenium and were further corroborated by theoretical studies (*vide infra*). The splitting pattern of the peripheral selenium is probably due to geminal ^2J Se−H coupling. The coupling constant observed for this splitting (40 Hz) is close to the reported values (∼50−56 Hz) for the ^2J Se−H coupling constant, where Se is a part of heterocyclic ring and is coupled with a vinylic hydrogen.[51] This was further confirmed by recording a proton decoupled ^{77}Se NMR spectrum where the split peaks appear as a single peak (Figure S8). Similarly, the ^{125}Te NMR spectrum of **36** showed two signals, one at 1132 ppm and the other broad one at 366.73 ppm, which could be resolved into two signals at 366.98 and 366.49 ppm with a coupling constant of 77 Hz. The ^{125}Te NMR chemical shift observed at 366.73 ppm is significantly upfield shifted in comparison to related ditelluride, bis[2-[1-(3,5-dimethylphenyl)-2-naphthyl]-4,5-dihydro-4,4-dimethyloxazole]ditelluride (427 ppm).[52] This is indicative of a more negative charge at the terminal tellurium atom. The splitting of the peaks may be due to the ^2J Te−H coupling. The coupling constant (77 Hz) is in

DOI: 10.1021/acs.joc.6b00173
J. Org. Chem. 2016, 81, 3214−3226

good agreement with the reported values for tellurophene (^2J Te−H; ∼87−100 Hz).[53] The electronic environment around selenium in 1,6-dioxa-6a-selenapentalene **35** is similar to the electronic environment around the selenium center of the cyclic arylselenenate esters.[22] 1,6-Dioxa-6a-tellurapentalene **37** showed ^{125}Te NMR signal at 1982 ppm. The chemical shift is upfield as compared to the related tellurenate ester **14** (2280 ppm).[27] In the ^{125}Te NMR spectrum of cyclic monotelluride **38**, the signal observed at 774 ppm is significantly downfield shifted in comparison to the reported value of [2-[1-(3,5-dimethylphenyl)-2-naphthyl]-4,5-dihydro-4,4-dimethyloxazole]phenyltelluride (670 ppm).[52] This considerable downfield shift in ^{125}Te NMR spectrum of **38** can be attributed to the fact that here Te is part of a six-membered ring and the delocalization of ring tellurium lone pair electrons into the π-framework, such as in the resonance form **38(a′)** (Figure 1).

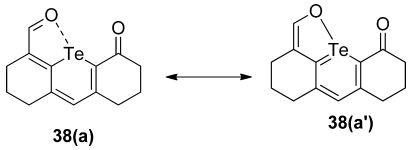

Figure 1. Resonance structures of compound **38**.

In ^{77}Se NMR spectrum of compound **39**, two expected ^{77}Se NMR signals were observed at 1190 and 1149.50 ppm corresponding to the two selenium atoms which are in the downfield region in comparison to the precursor **34** (884 and 502.58 ppm). The signal observed at 1149.50 ppm could be resolved into two peaks, 1149.86 and 1149.14 ppm with a coupling constant of 55 Hz. The ^{77}Se NMR signal for Se (selenium coordinated to oxygen) observed at 1190 ppm ($CDCl_3$) is close to the ^{77}Se NMR chemical shift reported for a seleninate ester[54] (1204 ppm (DMSO-d_6)) and of a seleninic acid anhydride[55] (1182 ppm (DMSO-d_6). Generally, the ^{77}Se NMR signals for aryl cyclic selenenate esters are observed in the range of 1350−1400 ppm. The observation of upfield shifted ^{77}Se NMR signals for **39**, which are in the range observed for seleninate esters, suggests that the possibility of the alternate structure **39a** is less likely. The ^{13}C NMR signal of formyl carbon is downfield (188.6 ppm) in comparison to the corresponding signal for1-oxa-6,6aλ^4-diselenapentalene **34** (181.3 ppm), while all three vinyl carbons are shifted to the upfield region (164.9, 138.2, 137.4 ppm) compared to **34** (168.5, 142.3, 142.2 ppm).

In the FT-IR spectra of compounds **33**, **34**, and **36**, the carbonyl stretching frequencies ($\nu_{C=O}$) were observed at 1597, 1577, and 1534 cm^{-1}, respectively. In general carbonyl groups of α,β-unsaturated aldehyde/ketone compounds display $\nu_{C=O}$ stretches in the range of 1666−1685 cm^{-1}. Therefore, the significant decrease in $\nu_{C=O}$ observed for **33**, **34**, and **36** is indicative of the presence of a strong E···O interaction in these compounds. Interestingly, the carbonyl stretching frequency ($\nu_{C=O}$) of 1-oxa-6,6aλ^4-dichalcogenopentalene systems decreases while going down the chalcogen group (S, Se, and Te). It is in direct correlation with the decreasing E···O bond distance (*vide infra*), in other words increasing E···O bond strength, along the chalcogen group. Due to the propensity of forming a strong E···O interaction while going down the chalcogen group,[15] the extent of donation of olefin π electrons into π^* orbital of C═O is higher for the tellurium system with respect to the systems containing its other lighter chalcogen congeners (Supporting Information, page S53). Therefore, increased electron density in the π^* orbital of C═O weakens its double-bond character, which concomitantly reduces the $\nu_{C=O}$ through the conjugation effect when there is strong E···O interaction. In cyclic telluride **38**, the $\nu_{C=O}$ of the formyl group was observed in lower stretching frequency region ($\nu_{C=O}$ 1519) as compared to $\nu_{C=O}$ of the ketone carbonyl group ($\nu_{C=O}$ 1635) and as well as to the $\nu_{C=O}$ of **33**, **34**, and **36**. This could be associated with the presence of stronger Te···O(CHO) interaction in **38** and resonance delocalization as described in Figure 1. The relatively higher $\nu_{C=O}$ observed for the ketone group in **38** with respect to the $\nu_{C=O}$ of formyl group in **36** and **38** is indicative of either weak or absence of four-membered Te···O(keto) interaction, which is consistent with the similar conclusion arrived from the studies on diaryl ditelluride systems (*vide infra*).[56]

X-RAY CRYSTALLOGRAPHIC STUDY

Molecular Structure of Compound 33. The molecular structure of compound **33** is depicted in Figure 2. The

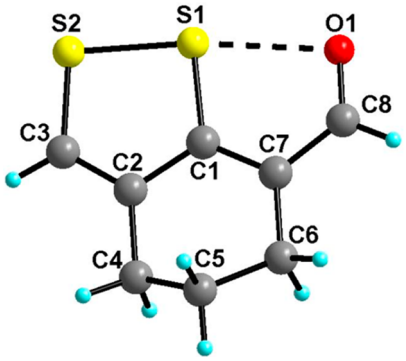

Figure 2. Molecular structure of **33**. Selected bond (Å) lengths and bond angles (deg): S1−S2 2.099(1), S1···O1 2.489(3), S1−S2−O1 172.96(8), C1−S1 1.741(3), C3−S2 1.721(3), C8−O1 1.241(4).

geometry around the sulfur S1 atom is T-shaped with S1−S2−O1 bond angle being 172.96(8)°, while the geometry around S2 is V-shaped in which S1 is covalently bonded to S2 and intramolecularly coordinated to O1 with S1···O1 bond distance of 2.489(3) Å. The S1···O1 bond distance (2.489(3) Å) is shorter than that reported for 2-(5-phenyl-1,2-dithiole-3-yl-idene)cyclohexanone (2.555(8)) Å[30] and slightly longer than the 2,5-dimethyl-dithiofurophthene (2.41 Å)[57] and 2,4-diphenyl-dithiofurophthene (2.382(6) Å.[58] However, the S−S bond (2.099(1) Å) is significantly shorter than the corresponding distance observed for 2-(5-phenyl-1,2-dithiole-3-yl-idene)-cyclohexanone (2.126(4)) Å,[30] 2,5-dimethyl-dithiofurophthene (2.12 Å), and 2,4-diphenyl-dithiofurophthene (2.106(3) Å). It is also slightly longer than the sum of S−S covalent radii (2.04 Å).[59] The planarity of the molecule is quite apparent from the torsion angles observed for the atoms defining the tricyclic ring system. All of the atoms forming fused five-membered rings are nearly coplanar with the torsion angles O1−C8−C7−C6 (179.6(3)°), S2−C3−C2−C4 (178.4(3)°), S1−S2−C3−C2 (0.3(3)°), C1−C7−C8−O1 (1.06(5)°) except C5, for which the torsional angle is C8−C7−C6−C5 is −156.3(3)°. Molecule **33** shows intermolecular hydrogen bonding (O···H) and S···S van der Waals interactions in the solid state (Figure S39). The O···H bond distances are 2.355(2) Å (O1···H3A) and 2.568(2)

DOI: 10.1021/acs.joc.6b00173
J. Org. Chem. 2016, 81, 3214−3226

Å (O1···H5A) with bond angles of C3−H3A···O1 (172.3(3)°) and C5−H5A···O1 (148.1(2)°).

Molecular Structure of 34. The coordination geometry around Se2 is V-shaped, while Se1 is approximately T-shaped (Figure 3) with bond angles C1−Se2−Se1 and Se2−Se1−O1

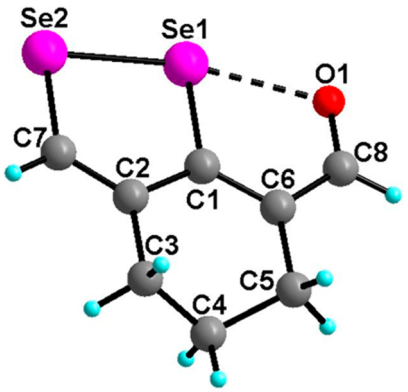

Figure 3. Molecular structure of **34**. Selected bond (Å) lengths and bond angles (deg): Se1···O1 2.392(11), Se1−C1 1.877(10), Se2−C7 1.839 (11), Se1−Se2 2.374(1), Se2−Se1−O1 168.4(1)°.

of 90.1(2)° and 168.4(1)°, respectively. The observed Se1−Se2 bond length of 2.374(1) Å is shorter than the respective Se−Se distances in related heterocycles, 3,4-dimethyl-1-oxa-6,6aλ^4-diselena-2-azapentalene[60] (2.444(2) Å) and 3,4-dimethyl-1-thia-6,6aλ^4-diselena-2-azapentalene (2.473(2) Å).[60] However, it is close to the distances reported for *peri*-substituted diselenides such as naphtho[1,8-*c*,*d*][1,2]diselenole[61] (2.364(5)Å), 2,7-di-*tert*-butylnaphtho[1,8-*c*,*d*][1,2]diselenole[62] (2.338(5) Å), and 2-*tert*-butylnaphtho[1,8-*c*,*d*][1,2]diselenole[62] (2.339(1)Å). The Se1···O1 bond length of 2.392(11) Å is longer than the observed for 3,4-dimethyl-1-oxa-6,6aλ^4-diselena-2-azapentalene[60] (Se−O (2.043(8) Å) and much shorter than those observed for bis(*o*-formylphenyl)diselenide with Se···O distances are in the range of 2.720−2.751 Å. The sum of the van der Waals radii of selenium and oxygen is 3.42 Å[63] which indicates a strong intramolecular Se···O interaction leading to the formation of a tricyclic ring system in similar to the 1-oxa-6,6aλ^4-dithiapentalene **33**. The torsion angles forming fused five-membered rings are O1−C8−C6−C5 (180°), Se2−C7−C2−C3 (180°), Se1−Se2−C7−C2 (0°), C1−C6−C8−O1 (0°), except C4, for which the torsion angle C8−C6−C5−C4 is −157°. Similar to **33**, the two-dimensional packing diagram of **34** shows weak Se···Se and O···H intermolecular interactions forming a one-dimensional chain network (Figure S40). The bond distances between Se1···Se1, Se2···Se2, and O···H are 3.529(9), 3.664(1), and 2.481(4) Å, respectively, and C7−H7A···O1 bond angle is 178°. The Se···Se noncovalent bond length is 3.529(9) Å, which is significantly shorter than the reported for selenenate ester **9a** (3.612(8) Å).[22]

Molecular Structure of 36. The molecular structure of **36** is represented in Figure 4. The intramolecular Te1···O1 distance (2.400(1) Å) is significantly shorter than those reported for a cyclic tellurenate ester **14**[27] (2.504 Å). The E−E···O (E = S, Se, Te) bond angles decrease while going from S to Te, with S(1)−S(2)−O(1), O(1)−Se(1)−Se(2), and O(1a)−Te(1a)−Te(2a) bond angles being 172.96(8)°, 168.4(1)°, and 159.6(6)°, respectively.

The packing diagram of **36**, revealed Te···Te and Te···O intermolecular interactions. Interestingly, two telluriums have

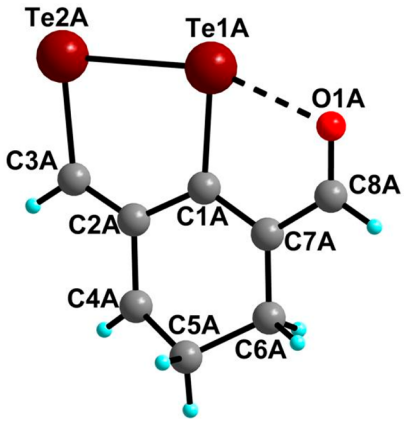

Figure 4. Molecular structure of **36**. Selected bond (Å) lengths and bond angles (deg): Te1···O1 2.400(1), Te1A−Te2A 2.758(3), O1A−Te1A−Te2A 159.6(6).

different modes of interactions. One of the telluriums, Te2 intermolecularly interacts with two tellurium atoms Te2 and Te1, while tellurium Te1 intramolecularly interacts with only one tellurium (Te2) of the neighboring molecule to construct a Te_4 rhombic core. The intermolecular interactions between Te2A···Te1A and Te2A···Te2A are 3.959 and 3.975 Å (Figure S41).

The structural elucidation of compounds **33**, **34**, and **36** shows that these molecules are nearly planar, except the carbon C4/C5 which has translational freedom of motion. This planarity can be interpreted in terms of the following resonating structures **a**−**c** (Figure 5), **a**/**b** with SBI O···E−E/O−E···E or **c**

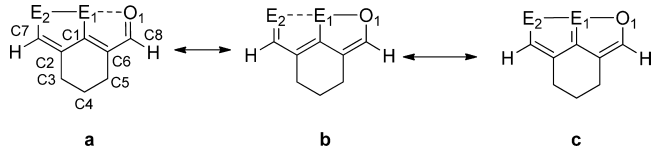

Figure 5. Possible resonance structures of 1-oxa-6,6aλ^4-dichalcogenopentalenes, **33**, **34**, and **36**.

with a covalent O−E−E bond. However, the X-ray structure analysis (Table 1) indicates 1-oxa-6,6aλ^4-diselenapentalene (**34**) to be more planar than 1-oxa-6,6aλ^4-dithiapentalene (**33**) and 1-oxa-6,6aλ^4-ditellurapentalene (**36**).

Molecular Structure of 35. The molecular structure of **35** is depicted in Figure 6. The asymmetric unit contains two independent molecules with almost similar bond lengths and bond angles. The geometry around selenium is T-shaped, where the Se is covalently bonded with two oxygen atoms. The Se−O bond distances of Se1−O1A (2.022(2) Å) and Se1−

Table 1. Comparison of X-ray Crystallographycally Obtained in-Plane Torsion Angles for 33, 34, and 36

	torsion angles (deg)		
torsion planes	33	34	36
C1−E1−E2−C7	−1.2(2)	0.0(3)	−0(1)
E1−E2−C7−C2	0.3(3)	0.0(6)	4(2)
E2−E1−C1−C2	2.0(2)	0.0(4)	−3(2)
E1−C1−C2−C7	−2.2(4)	0.0(8)	7(4)
E1−C1−C6−C8	−1.4(4)	−0.0(7)	0(3)
C1−C6−C8−O1	−1.1(5)	0.0(9)	−2(4)

DOI: 10.1021/acs.joc.6b00173
J. Org. Chem. 2016, 81, 3214−3226

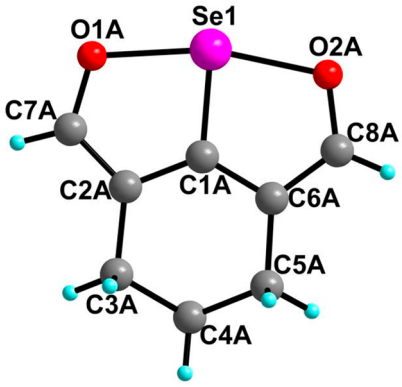

Figure 6. Molecular structure of **35**. Selected bond (Å) lengths and bond angles (deg): Se1−C1A 1.838(2), Se1−O1A 2.022(2), Se1−O2A 2.036(2), O1A−Se1−O2A 164.92(8).

O2A (2.036(2) Å) are in good agreement with the reported structure of **27**[39] (2.030 and 2.017 Å) but longer than Se−O covalent bond length of 1.871(2) Å reported for a selenenate ester.[22] The Se1−C1A bond distance 1.838(2) Å is similar to that reported for compound **27** (1.828 Å).[39] The molecular structure shows that two five-membered fused rings are nearly coplanar with the torsion angles of Se1−C1A−C6A−C5A −178.16(2)°, Se1−C1A−C2A−C3A −180°, O1A−C7A−C2A−C3A 179.7(3)°, O2−C8A−C6A−C5A −180(3)°. The packing diagram shows three different types of C−H···O intermolecular hydrogen-bonding interactions which give rise to a supramolecular assembly (Figure S42). The H···O bond distances are O2A···H8BA−C8B 2.756(8) Å, O2B···H7AA−C7A 2.528(7) Å, and O1B···H8AA−C8A 2.483(2) Å with the bond angles 154.0(22)°, 152.8(16)°, and 154.1(16)° respectively.

Molecular Structure of 37. 1,6-Dioxa-6a-tellurapentalene **37** (Figure 7) crystallizes in orthorhombic crystal system with

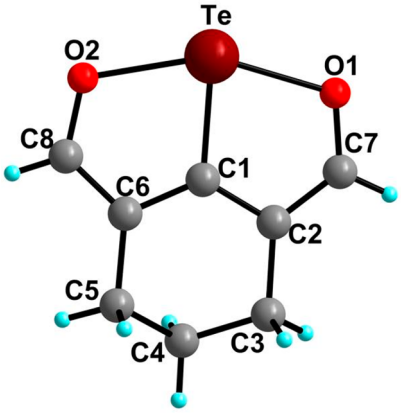

Figure 7. Molecular structure of **37**. Selected bond (Å) lengths and bond angles (deg): Te−O1 2.174(5), Te−O2 2.162(5), O2−Te−O1 154.17(19).

chiral space group $P2_12_12_1$, and the Flack parameter is 0.01(7). The geometry around tellurium is T-shaped with O1−Te−O2 bond angles of 154.17(19)°. The Te−O bond lengths 2.174(5) Å (Te−O1) and 2.162(5) Å(Te−O2) are in good agreement with reported tellurapentalene **29**,[43] having Te−O bond lengths of 2.130 and 2.124 Å. These are also very close to the Te−O bond length of compound **40** (2.074(3)) and reported values for tellurane **13b** (2.133 and 2.173 Å).[27]

The packing diagram of **37** shows weak intermolecular Te··· O1 and C4−H4B···O2 interactions with bond distances of 3.473(5) and 2.596(5) Å, respectively (Figure S43).

Molecular Structure of 40. The geometry around the tellurium atom is distorted T-shaped (Figure 8) with the bond

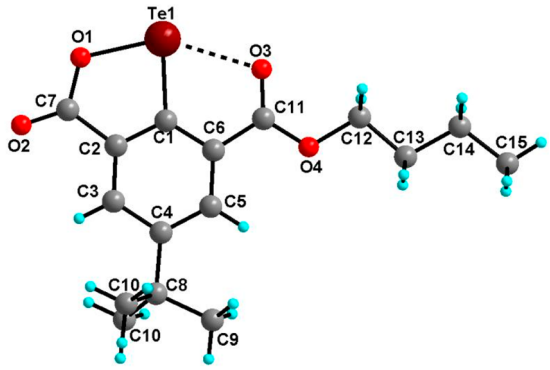

Figure 8. Molecular structure of **40**. Selected bond distances (Å) and bond angles (deg): Te1−O1 2.074(3), Te1···O3 2.548(3), Te1−C1 2.043(3), O3−Te−O1 149.9(10).

angle O1−Te−O3 of 149.9(10)° which is the good agreement with reported tellurenate ester **14**[27] (149.8°), however, it is significantly smaller than the respective bond angle observed for the alicylic analogue **37** (154°). In **40**, one of the oxygens is directly bonded to the Te atom, and another one is intramolecularly coordinated to tellurium. In **37**, both the oxygens are directly bonded (covalent bond) to the tellurium atom. The Te1−O1 bond distance 2.074(3) is shorter than the observed Te−O bond distances (2.174(5) and 2.162(5) Å) of alicyclic 1,6-dioxa-6a-tellurapentalene **37**. The intramolecular Te···O3 bond distance (2.548(3) Å) is close to the distance reported for related tellurenate ester **14**[27] (2.504 Å), however, it is longer than the distance observed for **36** (2.40 Å) and shorter than the distance observed for **38** (2.602(6) Å). The C−Te bond distance 2.043(3) Å is slightly longer than C−Te bond distance observed for **37** (2.020 (5) Å).

Molecular Structure of 38. In cyclic telluride **38** (Figure 9), the geometry around Te is V-shaped in which tellurium is strongly intramolecularly coordinated with the formyl oxygen (O2) and on the other side coordinated with ketonic oxygen (O1) with Te···O2 and Te···O1 bond distances of 2.602(6) and 3.006(6) Å, respectively. The Te···O bond distance for the five-membered ring is close to the value reported for related

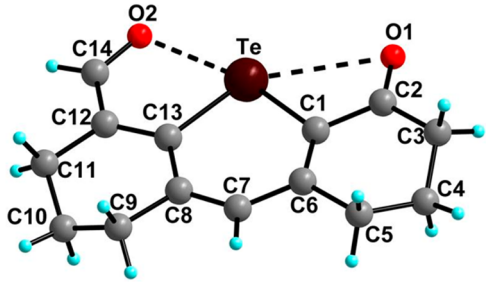

Figure 9. Molecular structure of **38**. Selected bond (Å) lengths and bond angles (deg): Te···O2 2.602(6), Te−O1 3.006(6), Te−C13 2.075(7), O2···Te−C1 166.3(3), C13−Te−C1 93.1(3).

DOI: 10.1021/acs.joc.6b00173
J. Org. Chem. 2016, 81, 3214−3226

3,4,5,6,7,8-hexahydro-2*H*-9-telluraanthracene-1-carbaldehyde 2.591(5)Å.[64] The crystal structure of compound **38** exhibits intermolecular Te···H and C−H···O interactions with Te−H5B and O1···H7A bond distances of 3.103(1) and 2.510(6) Å, respectively, while the Te···H−C and C−H···O bond angles are 149.94° and 157.04°, respectively (Figure S44).

COMPUTATIONAL STUDIES

The Role of E···O Interaction on Chalcogenopentalene Formation. As mentioned in the Synthesis section, the reactions of **16** with disodium dichalcogenides led to the formation of unsymmetrical chalcogenopentalenes (**33**, **34**, and **36**) and symmetrical (**35** and **37**) chalcogenopentalenes. The competing pathways that lead to the formation of unsymmetrical and symmetrical chalcogenopentalenes are outlined in Scheme 2. The formation of the unsymmetrical chalcogenopentalene is straightforward since the chalcogenolates have a strong propensity to react with conjugated dienophiles via intramolecular 1,6-conjugate addition reaction (Path (i)).[65]

Based on our previous observations on the intramolecular cyclization of 2,6-disubstituted arylchalcogen compounds, we speculated that the formation of the symmetrical chalcogenopentalenes could occur via the intramolecular nucleophilic attack of the hydroxyl group on the chalcogen center (Path (ii)).[23] To our surprise, this reaction occurs only for selenium and tellurium analogues but not for the sulfur analogue. To understand these phenomena, we carried out a conformational analysis on these systems using density functional theory (DFT) calculations. For brevity, the sodium ion has been exchanged with H^+ in the calculations. All the possible conformers of **a**−**c** ((syn, syn), (anti, syn), (syn, anti), and (anti, anti)) have been optimized (Figure 10). Where (syn, syn) and (anti, anti)

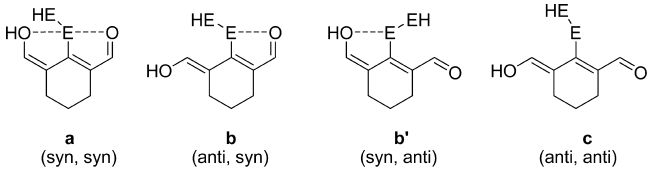

Figure 10. Possible conformers of chalcogenopentalenes.

conformation, both oxygens are either in a syn configuration or in an anti configuration with respect to the carbon to which the central chalcogen is bonded. Whereas, the (syn, anti) or (anti, syn) configuration refers the conformers in which one oxygen is in syn configuration and other one is in anti configuration with respect to the carbon to which the central chalcogen is bonded. The calculated relative electronic energies are provided in Table 2 and illustrated in Figure 11.

Table 2. Relative Electronic Energies

E	(syn, syn) = **a**	(anti, syn) = **b**	(syn, anti) = **b′**	(anti, anti) = **c**
S	7.30	4.94	7.10	0
Se	4.14	1.80	5.78	0
Te	2.89	0	7.13	3.74

The apparent features of the relative energy are: (i) For S and Se analogues, the relative energy of the conformers follows the order of **a** > **b′** > **b** > **c** and **b′** > **a** > **b** > **c**, respectively, and (ii) for the Te analogue, the relative energy of the conformers follows the order of **b′** > **c** > **a** > **b**. Based on these observations we can infer that the contribution of the hydroxyl functions E···O interaction toward stabilization is of least importance, and this is evident from the relatively higher energies of this conformation with respect to others. This corroborates with our previous observations that hydroxyl function are poorer electron donors than the carbonyl donors in terms of donor−acceptor interactions.[26,56] The conformers of our interests are **b** and **c**, as S and Se analogues prefer the **c** (anti, anti) geometry

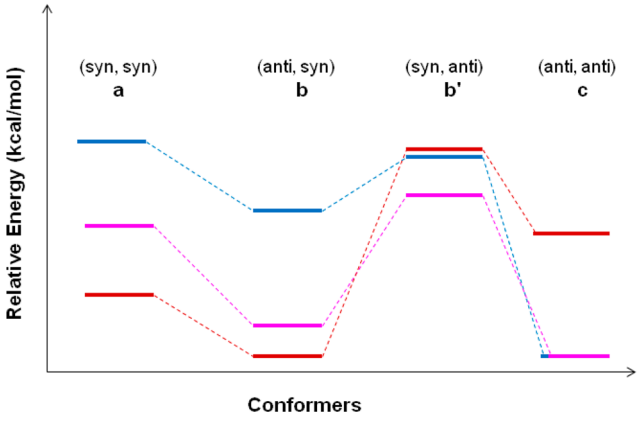

Figure 11. Blue is the sulfur analogue, pinkis the selenium analogue, and brown is the tellurium analogue.

and the Te analogue prefers the **b** (anti, syn) geometry. A close observation of the geometries of **b** (anti, syn) and **c** (anti, anti) conformers reveals that there is a disruption of the planarity of the conjugated olefinic bonds in conformers **b** and corresponding **c** conformers are highly planar along the conjugated olefinic bonds. The deviation from the planarity in conformers **b** could be due to the strict requirement of linearity of the donor−acceptor 3c-4e bond for the effective interaction. The obstruction or steric collision of this linear interaction elements by the second heteroatom donor leads to the distortion of planarity of the $\pi-\pi$ conjugated olefin bonds in conformers **b**. It reveals that there is competition between the two stabilizing forces, i.e., $\pi-\pi$ extended conjugation and intramolecular SBI. The $\pi-\pi$ conjugation seems to be the most dominant stabilization force for sulfur and selenium analogues, whereas the secondary bonding O···E interaction dominates in the case of tellurium analogue. The tellurium atom is more polarizable than the sulfur and selenium atom that leads to the favorable Te···O interaction. Therefore, the SBI must be sufficient enough to overcome the destabilization that arises from the small disruption of the extended π-conjugation system.

This intramolecular stabilization of the intermediate does not stop there, rather it activates the central tellurium toward intramolecular nucleophilic attack of the hydroxyl function by making the central tellurium more electrophilic. This leads to the formation of the symmetrical 1,6-dioxa-6a-tellurapentalene. In case of the selenium analogue, the energy of the conformer **b** is 1.80 kcal/mol higher than the conformer **c**. It is probable that this conformer could be populated at slightly elevated temperatures such that it leads to the formation of symmetrical 1,6-dioxa-6a-selenapentalene. However, for the sulfur analogue, electronic energy of conformation **b** is 4.94 kcal/mol higher than that of the energy of the conformation **c**. This ΔE ($= E_c - E_b$) is almost 3 times higher than that of the corresponding ΔE of the selenium conformers. This leads to predominant formation unsymmetrical thiapentalene **33** via exclusive thiolate addition reaction across the conjugated olefine and does not lead to the formation of symmetrical thiapentalene (sulfur analogue of **35** or **37**).

Natural Bond Orbital (NBO) Analysis. To gain more information about the intramolecular E···O (E = S, Se, Te) interaction in the newly synthesized organochalcogen compounds (**33**−**40**), DFT calculations have been carried out using Gaussian 09 suite of programs.[66] The gas-phase optimized geometries obtained by DFT calculations were well in conformity with the determined crystal structures of the respective compounds, except compound **39** where no crystal data is available (e.g., E···O distance, Table 3). The second-order perturbation energies for intramolecular E···O interactions obtained from NBO analysis[67−69] for compounds **33**−**40** are listed in Table 3. It indicates that the interaction energies in 1-oxa-6,6aλ^4-dichalcogenopentalenes **33**, **34**, and **36** increase while going from sulfur to tellurium. In the case of 1-oxa-6,6aλ^4-diselenapentalene-6,6aλ^4-dioxide (Se^{IV}) **39**, the intramolecular Se···O interactions energy

DOI: 10.1021/acs.joc.6b00173
J. Org. Chem. 2016, 81, 3214−3226

Table 3. Computed Geometry Parameters, NBO Second-Order Perturbation Energy and the Natural Charges Obtained for 33−40[a]

				NPA charge		
compd	$r_{E-O}/r_{E\cdots O}$ (Å) exp	$r_{E\cdots O}/r_{E-O}$ (Å) calcd	$E_{E\cdots O}$ (kcal/mol)	qE	qE′	qO
33	2.489(3)	2.324	21.24	0.357	0.141	−0.587
34	2.392(5)	2.262	37.71	0.479	0.153	−0.592
36	2.40(2)	2.304	39.62	0.592	0.159	−0.617
38	3.006(6)[b]	2.985[b]	2.49	0.838	–	−0.558
	2.602(6)[c]	2.488[c]	13.76			−0.589
39	-	2.633	8.95	1.138	1.039	−0.508
35	2.036(2)	2.034	–	0.836	–	−0.640
	2.036(2)	2.033				−0.640
37	2.174(5)	2.171	–	0.959	–	−0.670
	2.162(5)	2.173				−0.670
40	2.548	2.486	17.84	0.875	–	−0.582
	2.074(3)	2.073				

[a]E = central chalcogen; E′ = peripheral chalcogen. [b]Four-membered Te···O interaction. [c]Five-membered Te···O interaction.

(8.95 kcal/mol) is less as compared to the corresponding 1-oxa-6,6aλ^4-diselenapentalene **34** (37.71 kcal/mol). We have previously noted that Se···O interaction in the low-valent chalcogen Se^{II} system is much stronger than the corresponding interaction present in the high-valent chalcogen Se^{IV} system. This is due to the reduced polarizability of selenium valence shell electrons in the latter system.[23] Within NBO model, the computed off-diagonal Fock matrix element $F(i,j)$ or resonance integral value for O···Se interaction in **39** is two times lower than that of the corresponding $F(i,j)$ value computed for compound **34** (Supporting Information, page S52). The weaker orbital overlap in the former could be attributed to the increase of ionic character in the O···Se bonding. It is further supported by the results obtained in AIM analysis (*vide infra*). The plausible reason could be that although in the higher oxidation state the acceptor orbital energy is significantly lowered, the spatial extension is not enough for the strong orbital interaction. For compound **38**, both four and five-membered Te···O interactions were observed. However, the Te1···O1 interaction energy for four-membered interaction is small (2.49 kcal/mol) in comparison to the Te1···O2 five-membered interaction energy (13.76 kcal/mol). It indicates that the five-membered interaction is stronger than the four-membered interaction. The charges on the central chalcogen and the peripheral chalcogens were calculated using natural population analysis (NPA). The NPA charges on the central chalcogen atoms (E) in compounds **33**, **34**, and **36** were found to be +0.357, + 0.479 and +0.592, respectively, and these are significantly greater than the peripheral chalcogens (E′) (+0.141, + 0.153, and +0.158, respectively). The NPA charges on central chalcogenes among 1-oxa-6,6aλ^4-dichalcogenopentalenes increase while going down the group from sulfur (**33**; + 0.357) to tellurium (**36**; + 0.592). It is well established that strong intramolecular coordination between E···O leads to a significant increase in the positive charge on the central chalcogen. Similarly, in cases of symmetrical structures, 1,6-dioxa-6a-chalcogenopentalenes **35** and **37**, the NPA charge on 1,6-dioxa-6a-tellurapentalene **37** (+0.959) is greater than 1,6-dioxa-6a-selenapentalene **35** (0.836). The NPA charge of 1,6-dioxa-6a-tellurapentalene **37** (+0.959) is also significantly higher than the cyclic monotelluride **38** (+0.838) and aromatic system **40** (+0.875). Similarly, in case of 1-oxa-6,6aλ^4-diselenapentalene-6,6aλ^4-dioxide **39**, the NPA charges of selenium (+1.138, + 1.039) are significantly higher than the corresponding 1-oxa-6,6aλ^4-diselenapentalene **34** (0.479, 0.153), which is expected where both seleniums are bonded to oxygen atoms and in higher oxidation state (IV) as compared to the 1-oxa-6,6aλ^4-diselenapentalene **34** (Se^{II}).

Atoms In Molecule Analysis (AIM). The electron density (ρ), Laplacian ($\nabla^2\rho$), and total energy density (H) at the bond critical points (bcp) of E−O and E···O bonds were calculated using literature procedure.[70] The molecular graphs for the compounds **33**−**40** are given in Figures S52 and S53. The observation of bond critical points between chalcogen E (E = S, Se, and Te) and oxygen and high value of electron density (Table 4) is a signature of strong E···O intermolecular interaction, and it revealed some of expected patterns. The electron density at the bond critical point observed in unsymmetrical dichalcogenides increases from S to Te. The negative values of H observed for E···O interaction support the contribution of covalent character and in corollary with orbital interaction predicted by the NBO analysis. Although E···O interaction is predominantly covalent, the observation of positive value of Laplacian ($\nabla^2\rho$) at the bcp implies the fact that the considerable ionic contribution to the E···O interaction cannot be ruled out. Especially, O···Te bond in 1,6-dioxa-6a-tellurapentalene **37** has high ionic character which is in agreement with lowest second-order perturbation energy obtained for O···Te interaction in the NBO analysis of **37**. Similar observation has already been observed by Iwaoka and co-workers[71] and Behera and co-workers[72] for Se···N intramolecular interactions. It has also been observed for Se···O intramolecular interactions.[67,73] In case of **39**, the value of total energy density (H) is positive (0.0006), and the Laplacian ($\nabla^2\rho$) at the bcp is very high which indicates predominant ionic character arising due to the higher oxidation state of the selenium in **39**. In compound **38**, no bcp could be located for the four-membered Te···O(keto) interaction. Whereas, the five-membered Te···O contact showed a bcp with an electron density (ρ) value of 0.042 au. It indicates the absence of four-membered Te···O interaction which is in accordance with very low second-order perturbation energy obtained in NBO analysis. Therefore, short Te···O contact observed in both solid state and gas-phase structures for the four-membered interaction could be a result of geometrical constraints rather than orbital interaction. The analysis further correlated with our earlier

Table 4. Selected Topographical Features of E···O Bonds Computed at the WTBS level for S, Se, and Te and MPW1PW91/6-311g(d,p) Level for C, H, O[a]

	ρ^b_{bcp}	$\nabla^2\rho^c_{bcp}$	H^d
compd	E···O/E−O	E···O/E−O	E···O/E−O
33	0.0471	0.1570	−0.0012
34	0.0567	0.1678	−0.0055
36	0.0575	0.0175	−0.0074
38	0.0422	0.1279	−0.0028
39	0.0293	9.4746	0.0006
40	0.0864	0.0852	−0.0147
35	0.0853, 0.0850	0.2175, 0.2169	−0.0206, −0.0820
37	0.0712, 0.0715	0.2545, 0.256	−0.0105, −0.0106

[a]bcp = bond critical point. [b]ρ = electron density at bcp. [c]$\nabla^2\rho$ = Laplacian at bcp. [d]H = total energy density.

DOI: 10.1021/acs.joc.6b00173
J. Org. Chem. 2016, 81, 3214−3226

observation on the absence of a weak intramolecular interaction in four-membered Te···O system.[56]

Nucleus Induced Chemical Shift (NICS). In order to understand the aromatic character of the two fused five-membered heterocyclic rings, the NICS were calculated.[74] One of the contributing forms of the resonance structures, that is shown in Figure 12, illustrates the

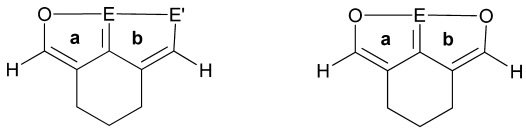

33 E = E' = S; **34** E = E' = Se; **36** E = E' = Te

35 E = Se; **37** E = Te

Figure 12. 1-Oxa-6,6aλ^4- and 1,6-dioxa-6a-chalcogenopentalenes rings.

aromatic $4n + 2$ π-electron system where each peripheral chalcogen contributes a pair of electrons to satisfy the Hückel's rule of aromaticity. The other resonance structures involving no bond resonance are shown in Figure 5. The isotropic chemical shifts (Table 5) were computed for the ghost atom (bq) placed at the middle of the rings **a** and **b**, NICS(0) (Figure 12). The calculation was also done by placing the ghost atom 1 Å above the plane, $NICS_{zz}(1)$ and below the plane, $NICS_{zz}(-1)$.

The isotropic chemical shift calculated in the plane includes the σ contributions as well. Whereas the isotropic chemical shift computed 1 Å above or below provides an idea of the extent of π electron delocalization and aromatic character. The isotropic chemical shifts ($NICS_{zz}(1)$) computed for the rings **a** and **b** in 1-oxa-6,6aλ^4-dichalcogenopentalenes (**33**, **34**, **36**) are not equal, which is in accordance with asymmetric nature of these molecules. However, it is worth noting that the isotropic chemical shift of five-membered **b** heterocyclic ring in compounds **33** (−7.14), **34** (−7.50), **36** (−6.08) is lower than the corresponding five-membered **a** ring. It could be due to the dominant p characters of the S and Se lone pairs that participate in delocalization within the **b** heterocyclic rings. The negative values and considerable nearness to the isotropic chemical shift value calculated for the benzene ring[75] (−11.304 ppm) indicates that the **b** rings in **33**, **34**, and **36** have substantial aromatic characters. Similarly, for 1,6-dioxa-6a-chalcogenopentalenes **35** and **37**, due to symmetrical structures of the heterocyclic rings **a** and **b**, the isotropic values ($NICS_{zz}$ (1)) are equal, i.e., −7.21 ppm (**35**) and −6.23 ppm (**37**), respectively. Compounds **39** and **40** have significantly higher isotropic chemical shift than the isotropic shift values of chalcopentalene derivatives. The molecular orbital diagrams generated using DFT calculation also revealed that the certain HOMOs of the chalcopentalene derivatives have delocalized electron density over the all the atoms, for example, HOMO−11 of **35** and HOMO−3 of **37**, of condensed heterocyclic ring system (Table S5).

CONCLUSIONS

In conclusion, 2-chlorocyclohex-1-ene-1,3-dicarbaldehyde (**16′**) and its enol form 2-chloro-1-formyl-3-hydroxymethylenecyclohexene (**16**) serve as excellent precursors for the one-pot synthesis of a series of chalcogenopentalenes. The potential repulsive interaction among the juxtaposed chalcogen atoms facilitates either nucleophilic attack of the hydroxyl function on the central electrophilic chalcogen or 1,6-addition followed by elimination to give 1,6-dioxa-6aλ^4-chalcogenopentalenes and 1-oxa-6,6aλ^4-dichalcogenopentalenes, respectively. The formation of 1-oxa-6,6aλ^4−dichalcogenopentalenes is favored due to strong propensity of chalcogenolates to react with conjugated dienophiles via intramolecular 1,6-conjugate addition reaction. However, the formation of 1,6-dioxa-6a-chalcogenopentalenes **35** and **37** results when the intramolecular E···O interaction is significant and is comparable to the stabilization due to $\pi-\pi$ conjugation. Among 1-oxa-6,6aλ^4-dichalcogenopentalenes, the intramolecular E···O interaction is strongest for the tellurium analogue **36**, and as expected the C═E character is more dominant for S analogue **33**. Although the NICS calculations show some aromatic character in chalcogenopentalene systems, this has to be rigorously evaluated in terms of their aromatic-like chemical reactivity to further support this view. Hence, these results will stimulate further attraction in the area of chalcogenopentalene chemistry. The synthetic procedure and the unique reactivity of the chalcogenolate intermediates reported in this work can be a useful method to synthesis of other substituted chalcogenopentalene derivatives for material application.

EXPERIMENTAL SECTION

All the organochalcogen derivatives were synthesized under nitrogen or argon atmosphere using standard Schlenk line techniques. Solvents were purified and dried by standard procedures and were freshly distilled prior to use.[76] All the chemicals used were reagent grade and were used as received. Melting points were recorded in capillary tubes. The ^{1}H (400 MHz/500 MHz), ^{13}C (100/125 MHz), ^{77}Se (76.4/95.4 MHz), and ^{125}Te (126.3/157.8 MHz) NMR spectra were recorded in $CDCl_3$ solvent using NMR spectrometer. Chemical shifts cited were referenced with respect to TMS for (^{1}H and ^{13}C) as an internal standard and Me_2Se (for ^{77}Se) and Me_2Te (for ^{125}Te) as an external standards. Elemental analysis was performed on elemental analyzer. The IR spectra were recorded in the range of 400−4000 cm^{-1} by using KBr pellets for solid samples on a FT-IR spectrometer. Mass spectral (MS) studies were performed by using a Q-TOF Micro mass spectrometer with electrospray ionization (ESI) mode analysis. In the case of isotopic patterns, the value is given for the most abundant peak. In column chromatography, silica gel was used as a stationary phase, whereas petroleum ether (60−80 °C) and ethyl acetate were used as mobile phase.

Synthesis of 2-Chloro-1-formyl-3-hydroxymethylenecyclohexene (16).[45] To a cold solution of DMF (20 mL, 0.27 mol) in CH_2Cl_2 (20 mL), $POCl_3$ (18.5 mL, 0.115 mol) was added dropwise at 0 °C. After 30 min, cyclohexanone (5 g, 0.05 mol) was added at the same temperature. The resulting mixture was refluxed for 3 h at 58−60 °C. The reaction mixture was then cooled using ice bath, poured on

Table 5. Comparison of Isotropic Chemical Shifts Obtained for the Ghost Atom (bq) at the Center: In Plane NICS(0), Out of Plane $NICS_{zz}(1)$, and $NICS_{zz}(-1)$

compd	NICS(0), ppm		$NICS_{zz}(1)$, ppm		$NICS_{zz}(-1)$, ppm	
33	−10.627	−5.552	−7.141	−5.378	−7.437	−5.504
34	−10.172	−7.049	−7.500	−6.276	−7.879	−6.434
36	−8.790	−7.263	−6.075	−6.029	−6.375	−6.111
35	−9.298	−9.307	−7.205	−7.208	−7.599	−7.602
37	−8.430	−8.424	−6.227	−6.227	−6.576	−6.575
39	−2.485	−0.686	−3.221	−3.197	−3.261	−2.267
40	−4.406	−2.927	−2.485	−2.477	−2.485	−2.477
Benzene	−8.960	–	−11.304	–	−11.304	–

DOI: 10.1021/acs.joc.6b00173
J. Org. Chem. 2016, 81, 3214−3226

crushed ice, and kept for 1−2 h. The resulting yellow precipitate was collected and washed with cold water (partially soluble in water) to remove the acidic impurities and finally washed with cold ethanol. Yield: 8.0 g, (91%); mp 126−128 °C (lit.125−127 °C); ^{1}H NMR (400 MHz, CD_3OD): δ(ppm) 10.16 (s, 1H) 7.26 (s, 1H), 2.57−2.41 (m, 2H), 1.67−1.57 (m, 2H); FT-IR (KBr) $\upsilon_{C=O}$, 1603; CH−OH, 3198 cm^{-1}. MS-ESI: m/z calcd for $C_8H_{10}ClO_2$: 173.0, found: 173.1 [M + H]$^+$.

Synthesis of 1-Oxa-6,6aλ^4-dithiapentalene 33. A stirred solution of disodium disulfide [prepared *in situ* by the reaction of sodium (0.84 g, 0.037 mol) and sulfur (1.16 g, 36.5 mmol) in dry THF in the presence of catalytic amount of naphthalene][77] was treated with **16** (5.92 g, 34.4 mmol) and HMPA (14.6 mL) at room temperature. The reaction mixture was stirred at room temperature for 1 h and then refluxed for 4 h. After cooling, the reaction mixture was poured into water, and the organic layer was extracted with dichloromethane, washed twice with water, and dried over Na_2SO_4. The resulting solution was concentrated under vacuum to get as a yellow orange liquid. The liquid was purified by column chromatography (1−3% ethyl acetate-petroleum ether) to get **33** as a yellow solid which was recrystallized from slow evaporation of ethyl acetate-*n*-hexane to give a yellow color needles. Yield: 2.31g (37%), mp 108−109 °C; ^{1}H NMR (400 MHz, $CDCl_3$): δ(ppm) 9.33 (s, −CHO, 1H), 7.50 (s, 1H), 2.85−2.81 (m, 2H), 2.71−2.68 (t, 2H, J = 6 Hz), 1.93−1.88 (m, 4H); ^{13}C NMR ($CDCl_3$): δ 21.1, 24.8, 28.3, 121.0, 137.3, 137.4, 163.2, 182.5; FT-IR (KBr) υ 812, 1064, 1369, 1418, 1440, 1597, 2933, 3010 cm^{-1}. HRMS-ESI: m/z calcd for $C_8H_9S_2O$: 185.0095, found: 185.0098 [M + H]$^+$.

Synthesis of 1-Oxa-6,6aλ^4-diselenapentalene 34. A solution of disodium diselenide [generated *in situ* from the mixture of sodium (0.07 g, 3 mmol) and selenium (0.24 g, 3.0 mmol) in dry THF in the presence of catalytic amount of naphthalene][77] was treated with **16** (0.50 g, 2.9 mmol) in HMPA (1.19 mL, 6.67 mmol) at room temperature. The reaction mixture was stirred at room temperature for 1 h and then refluxed for 6 h. After cooling, the reaction mixture was poured into water. The organic layer was extracted with dichloromethane and washed twice with water, dried over Na_2SO_4, and concentrated under vacuum to get an orange liquid. The liquid was purified by column chromatography (2−5% ethyl acetate-petroleum ether) to get four fractions. The first fraction was 1-oxa-6,6aλ^4-diselenapentalene **34** as an orange solid. The second fraction was 1,6-dioxa-6a-selenapentalene **35** as a yellow colored solid, and the third fraction was as a maroon colored sticky solid which could not be characterized. The compounds were recrystallized from ethyl acetate and *n*-hexane.

*1-Oxa-6,6aλ^4-diselenapentalene (**34**).* Orange solid; yield: 0.18 g (21%), mp 94−96 °C; ^{1}H NMR (400 MHz, $CDCl_3$): δ(ppm) 9.45 (s, −CHO, 1H), 8.37 (s, 1H), 2.92−2.89 (t, 2H, J = 5.8 Hz), 2.63−2.60 (t, 2H, J = 5.8 Hz), 1.99−1.93 (m, 2H); ^{13}C NMR (100 MHz, $CDCl_3$): δ 22.1, 26.0, 31.3, 127.4, 142.2, 142.3, 168.5, 181.2, 181.3; ^{77}Se NMR (95.4 MHz, $CDCl_3$): δ 884, 502.58 (^2J Se−H, 40 Hz); FT-IR (KBr) υ 820, 857, 1356, 1412, 1428, 1577, 2936, 3017 cm^{-1}. HRMS-ESI: m/z calcd for $C_8H_9Se_2O$: 280.8984, found: 280.8986 [M + H]$^+$; Anal. calcd for $C_8H_8Se_2O$: C, 34.55; H, 2.90; found C, 34.55, H, 2.75.

*1,6-Dioxa-6a-selenapentalene (**35**).* Yellow solid; yield: 0.16 g (26%), mp 99−101 °C; ^{1}H NMR (400 MHz, $CDCl_3$): δ (ppm) 8.70 (s, 2H), 2.85−2.82 (t, 4H, J = 5.9 Hz), 2.01−1.97 (m, 2H); ^{13}C NMR (100 MHz, $CDCl_3$): 22.6, 23.0, 117.8, 167.3, 173.4; ^{77}Se NMR (76.4 MHz, $CDCl_3$): δ 1379; HRMS-ESI: m/z calcd for $C_8H_9SeO_2$: 216.9763; found: 216.9771 [M + H]$^+$. FT-IR (KBr) υ 665, 1190, 1227, 1325, 1421, 1437, 1542, 2836, 2866 2937 cm^{-1}. Anal. calcd for $C_8H_8SeO_2$: C, 44.67, H, 3.75; found: C, 44.54, H, 3.41.

Synthesis of 1-Oxa-6,6aλ^4-ditellurapentalene 36. A stirred solution of disodium ditelluride [generated *in situ* by the mixture of sodium (0.33 g, 14 mmol) and tellurium (1.82 g, 14.3 mmol) in dry THF in the presence of catalytic amount of naphthalene][77,78] was reacted with **16** (2.5 g, 14 mmol) in HMPA (5.7 mL) at room temperature. The mixture was stirred for 1 h at room temperature and then refluxed for 6 h. After cooling, the reaction mixture was poured into ice−water mixture. The organic layer was extracted with dichloromethane and washed with cold water twice, dried over Na_2SO_4, and concentrated under vacuum to get a deep red-orange liquid. The liquid was purified by column chromatography (2−10% ethyl acetate-petroleum ether). Similarly, in the case of Na_2Te_2 reaction, four fractions were obtained. The first fraction isolated was 1-oxa-6,6aλ^4-ditellurapentalene **36** as red colored solid, and the second fraction was 1,6-dioxa-6a-tellurapentalene **37** as yellowish orange colored solid. The third fraction was cyclic monotelluride **38** as a dark red solid, and fourth one was the unreacted starting material **16**. The crystals were obtained from dichloromethane-*n*-hexane by slow evaporation.

*1-Oxa-6,6aλ^4-ditellurapentalene (**36**).* Red solid; yield: 0.24 g (5%), mp 116−118 °C; ^{1}H NMR (400 MHz, $CDCl_3$): δ(ppm) 9.97 (s, −CHO, 1H), 9.88 (s, −CHO, 1H), 3.16−3.13 (t, 2H, J = 5.9 Hz), 2.53−2.51 (t, 2H, J = 6.0 Hz), 2.04−1.96 (m, 2H); ^{13}C NMR (125.8 MHz, $CDCl_3$): δ 22.6, 28.0, 35.7, 134.5, 135.2, 155.5, 164.8, 179.7; ^{125}Te NMR (157.8 MHz, $CDCl_3$): δ 1132, 366.73 (^2J Te−H 77 Hz); FT-IR (KBr) υ 664, 1058, 1177, 1299, 1396, 1432, 1534, 1632, 2920. HRMS-ESI: m/z calcd for $C_8H_9Te_2O$: 380.8778; found: 380.8761 [M + H]$^+$.

*1,6-Dioxa-6a-tellurapentalene (**37**).* Yellowish orange solid; yield: 0.75 g (20%), mp 125−127 °C; ^{1}H NMR (400 MHz, $CDCl_3$): δ(ppm) 9.02 (s, 2H), 2.91−2.88 (t, 4H, J = 5.9 Hz), 2.03−1.97 (quintet, 2H, J = 6.2 Hz); ^{13}C NMR (100 MHz, $CDCl_3$): δ 23.0, 24.9, 123.0, 135.2, 170.4, 172.4; ^{125}Te NMR (126 MHz, $CDCl_3$): δ 1982; FT-IR (KBr) υ 656, 644, 1177, 1218, 1236, 1410, 1434, 1533, 1656, 2922, cm^{-1}. HRMS-ESI: m/z calcd for $C_8H_9TeO_2$: 266.9665, found: 266.9657 [M + H]$^+$. Anal. calcd for $C_8H_9TeO_2$: C, 36.43; H, 3.06; found C, 36.59; H, 2.91.

*Cyclic monotelluride **38**.* Dark red solid; Yield: 0.33 g (7%), mp 179−181 °C; ^{1}H NMR (400 MHz, $CDCl_3$): δ(ppm) 9.94 (s, 1H), 6.68 (s, 1H), 2.89−2.85 (t, 2H, J = 5.5 Hz), 2.72−2.61 (m, 4H), 2.16−2.09 (quintet, 4H, J = 5.9 Hz), 2.04−1.91 (m, 2H); ^{13}C NMR (100 MHz, $CDCl_3$): δ 22.0, 22.9, 34.0, 36.1, 37.4, 131.7, 137.2, 141.1, 145.3, 152.1, 188.4, 200.3; ^{125}Te NMR (126 MHz, $CDCl_3$): δ 774; FT-IR (KBr) υ 705, 982, 987, 1171, 1188, 1415, 1435, 1519, 1606, 1635, 2939; MS-ESI m/z calcd for $C_{14}H_{15}TeO_2$: 345.01, found: 345.01 [M + H]$^+$. Anal. calcd for $C_{14}H_{14}TeO_2$: 49.19; H, 4.13; found C, 49.63; H, 4.41.

Synthesis of 1-Oxa-6,6aλ^4-diselenapentalene-6,6aλ^4-dioxide 39. A solution of *m*-chloroperbenzoic acid (0.25 g, 0.72 mmol) in dry dichloromethane (7 mL) was cooled to −73 °C. To the above was added 1-oxa-6,6aλ^4-diselenapentalene **34** (0.10 g, 0.36 mmol), and the reaction was allowed to stir at this temperature for 35 to 40 min. Then the reaction mixture was poured into the solution containing saturated $NaHCO_3$ and dichloromethane. The organic layer was extracted with dichloromethane, washed thrice with water, and dried over Na_2SO_4. The filtrate was concentrated and washed with hexane to get **39** as an orange yellow solid. Yield: 0.02 g (15%), mp 126−128 °C; ^{1}H NMR (400 MHz, $CDCl_3$): δ(ppm) 9.70 (s, −CHO, 1H), 6.95 (s, 1H), 3.00−2.81 (m, 2H), 2.77−2.60 (m, 2H), 2.17−1.93 (m, 2H); ^{13}C NMR (100.6 MHz, $CDCl_3$): δ 22.3, 26.1, 35.6, 130.7, 137.4, 138.2, 164.9, 188.6; ^{77}Se NMR (76.4 MHz, $CDCl_3$): δ 1190, 1149.49 (^2J Se−H, 55 Hz); HRMS-ESI: m/z calcd for $C_8H_9Se_2O_3$: 312.8882, found: 312.8889 [M + H]$^+$.

Computational Details. All calculations were performed with Gaussian 09 program.[66] Geometries were fully optimized at MPW1PW91 method by using Lanl2dz(d,p) basis set for sulfur, selenium, and tellurium and 6-311g(d,p) level for the rest of the atom. The NBO[67−69] and NICS[74] analyses for all the systems **33**−**39** were performed at MPW1PW91 method by using TZP-DKH basis set for sulfur, selenium, and tellurium and 6-311g(d,p) level for the rest of the atom. The AIM[66,79−81] analysis was performed with AIM[82] at MPW1PW91 level of theory with wtbs basis set for S, Se, and Te and 6-311g(d,p) level for remaining atoms.

X-ray Crystal Structure Determination. The single crystal X-ray diffraction measurements for compounds and **33**−**38** and **40** were performed on a diffraction measurement device with graphite monochromated Mo Kα radiation (λ = 0.7107 Å). The structures

DOI: 10.1021/acs.joc.6b00173
J. Org. Chem. 2016, 81, 3214−3226

were determined by routine heavy-atom method using SHELXS 97[83] and refined by full-matrix least-squares with the nonhydrogen atom anisotropic and hydrogen atoms with fixed isotropic thermal parameters of 0.07 Å by means of SHELXS 97 program.[84] The heteroatom hydrogens were located from difference electron density map, and the rest was fixed at predetermined positions. Scattering factors were from common sources.[85] A riding model was chosen for refinement. The structure refinement parameters for compounds **33**–**38** and **40** are given in Tables S1 and S2. CCDC-1012745 (**33**), CCDC-1012749 (**34**), CCDC-1012744 (**35**), CCDC- 1012746 (**36**), CCDC-1012748 (**37**), CCDC-1012747 (**38**), and CCDC-1012750 (**40**) contain the supplementary crystallographic datafor this paper. These data can be obtained free of charge from The Cambridge Crystallographic Data Centre via www.ccdc.cam.ac.uk/data_request/cif.

■ ASSOCIATED CONTENT

Supporting Information

The Supporting Information is available free of charge on the ACS Publications website at DOI: 10.1021/acs.joc.6b00173.

^{1}H, ^{13}C, ^{77}Se and ^{125}Te NMR spectra, MS (ESI) or HRMS (ESI), DFT-optimized geometries, ORTEP diagrams, unit cell packing diagrams and tables of crystal refinement data for compounds **33**, **34**, **35**, **36**, **37**, **38**, and **40** (PDF)

Crystallographic data for **33** (CIF)

Crystallographic data for **34** (CIF)

Crystallographic data for **35** (CIF)

Crystallographic data for **36** (CIF)

Crystallographic data for **37** (CIF)

Crystallographic data for **38** (CIF)

Crystallographic data for **40** (CIF)

■ AUTHOR INFORMATION

Corresponding Author

*E-mail: chhbsia@chem.iitb.ac.in.

Notes

The authors declare no competing financial interest.

■ ACKNOWLEDGMENTS

H.B.S. is grateful to the Department of Science and Technology (DST), New Delhi (India), for J C Bose Fellowship. P.R.P. is thankful to Department of Chemistry, IIT Bombay for a teaching assistantship and to Dr. Sagar Sharma for help in computational studies.

■ DEDICATION

Dedicated to Professor Vladimir I. Minkin on the occasion of his 80th birthday.

■ REFERENCES

(1) Fujihara, H.; Mima, H.; Furukawa, N. *J. Am. Chem. Soc.* **1995**, *117*, 10153.

(2) Klapötke, T. M.; Krumm, B.; Polborn, K. *J. Am. Chem. Soc.* **2004**, *126*, 710.

(3) Nakanishi, W.; Hayashi, S.; Itoh, N. *J. Org. Chem.* **2004**, *69*, 1676.

(4) Sarma, B. K.; Mugesh, G. *J. Am. Chem. Soc.* **2005**, *127*, 11477.

(5) Sarma, B. K.; Mugesh, G. *Chem. - Eur. J.* **2008**, *14*, 10603.

(6) Back, T. G. *Organoselenium Chemistry: A Practical Approach*; Oxford University Press: Oxford, U.K., 1999.

(7) Nishibayashi, Y.; Uemura, S. *Top. Curr. Chem.* **2000**, *208*, 201.

(8) Back, T. G.; Kuzma, D.; Parvez, M. *J. Org. Chem.* **2005**, *70*, 9230.

(9) Khokhar, S. S.; Wirth, T. *Angew. Chem., Int. Ed.* **2004**, *43*, 631.

(10) Freudendahl, D. M.; Shahzad, S. A.; Wirth, T. *Eur. J. Org. Chem.* **2009**, *2009*, 1649.

(11) Kornienko, A.; Banerjee, S.; Kumar, G. A.; Riman, R. E.; Emge, T. J.; Brennan, J. G. *J. Am. Chem. Soc.* **2005**, *127*, 14008.

(12) Zhang, H.; Wang, D.; Möhwald, H. *Angew. Chem., Int. Ed.* **2006**, *45*, 748.

(13) Back, T. G.; Moussa, Z.; Parvez, M. *Angew. Chem., Int. Ed.* **2004**, *43*, 1268.

(14) Engman, L.; Stern, D.; Cotgreave, I. A.; Andersson, C. M. *J. Am. Chem. Soc.* **1992**, *114*, 9737.

(15) Mukherjee, A. J.; Zade, S. S.; Singh, H. B.; Sunoj, R. B. *Chem. Rev.* **2010**, *110*, 4357.

(16) Saiki, T.; Goto, K.; Okazaki, R. *Angew. Chem., Int. Ed. Engl.* **1997**, *36*, 2223.

(17) Kersting, B.; DeLion, M. *Z. Naturforsch., B: J. Chem. Sci.* **1999**, *54*, 1042.

(18) Kersting, B. *Z. Naturforsch.* **2002**, *57b*, 1115–1119.

(19) Zade, S. S.; Panda, S.; Tripathi, S. K.; Singh, H. B.; Wolmershauser, G. *Eur. J. Org. Chem.* **2004**, *18*, 3857.

(20) Roy, G.; Mugesh, G. *J. Am. Chem. Soc.* **2005**, *127*, 15207.

(21) Zade, S. S.; Panda, S.; Singh, H. B.; Sunoj, R. B.; Butcher, R. J. *J. Org. Chem.* **2005**, *70*, 3693.

(22) Selvakumar, K.; Singh, H. B.; Butcher, R. J. *Chem. - Eur. J.* **2010**, *16*, 10576.

(23) Singh, V. P.; Singh, H. B.; Butcher, R. J. *Chem. - Asian J.* **2011**, *6*, 1431.

(24) Parnham, M. J.; Biederman, J.; Bittner, C.; Dereu, N.; Leyck, S.; Wetzig, H. *Agents Actions* **1989**, *27*, 306.

(25) McNeil, N. M. R.; Matz, M. C.; Back, T. G. *J. Org. Chem.* **2013**, *78*, 10369.

(26) Selvakumar, K.; Singh, H. B.; Goel, N.; Singh, U. P.; Butcher, R. J. *Dalton Trans.* **2011**, *40*, 9858.

(27) Selvakumar, K.; Singh, H. B.; Goel, N.; Singh, U. P. *Organometallics* **2011**, *30*, 3892.

(28) Geiger, T.; Benmansour, H.; Fan, B.; Hany, R.; Nüesch, F. *Macromol. Rapid Commun.* **2008**, *29*, 651.

(29) Beer, R. J. S.; Poole, A. J. *Tetrahedron Lett.* **1972**, *13*, 1835.

(30) Pinel, R.; Mollier, Y.; Liaguno, E. C.; Paul, I. C. *J. Chem. Soc. D* **1971**, 1352.

(31) Reid, D. H.; Webster, R. G. *J. Chem. Soc., Perkin Trans. 1* **1972**, 1447.

(32) Minkin, V. I.; Minyaev, R. M. *Chem. Rev.* **2001**, *101*, 1247.

(33) Reid, D. H. *Organic Compounds of Sulphur, Selenium, and Tellurium*; The Chemical Society: London, 1970; Vol. *I*, pp 321–335.

(34) Chuang, Y.-C.; Li, Y.-W.; Hsu, I. J.; Lee, G.-H.; Wang, Y. *Inorg. Chem.* **2013**, *52*, 10958.

(35) Dingwall, J. G.; Reid, D. H.; Symon, J. D. *J. Chem. Soc. C* **1970**, 2412.

(36) Hansen, L. K.; Hordvik, A. *J. Chem. Soc., Chem. Commun.* **1974**, *0*, 800.

(37) Ingold, K. U.; Reid, D. H.; Walton, J. C. *J. Chem. Soc., Perkin Trans. 2* **1982**, 431.

(38) Christie, R. M.; Reid, D. H.; Walker, R.; Webster, R. G. *J. Chem. Soc., Perkin Trans. 1* **1978**, 195.

(39) Reid, D. H.; Webster, R. G. *J. Chem. Soc., Perkin Trans. 1* **1975**, 775.

(40) Dingwall, J. G.; Dunn, A. R.; Reid, D. H.; Wade, K. O. *J. Chem. Soc., Perkin Trans. 1* **1972**, 1360.

(41) Saethre, L. J.; Martensson, N.; Svensson, S.; Malmquist, P. A.; Gelius, U.; Siegbahn, K. *J. Am. Chem. Soc.* **1980**, *102*, 1783.

(42) Reid, D. H.; Webster, R. G. *J. Chem. Soc., Chem. Commun.* **1972**, 1283.

(43) Detty, M. R.; Luss, H. R. *J. Org. Chem.* **1983**, *48*, 5149.

(44) Detty, M. R.; Perlstein, J. H. Chalcogenopentalene Compounds in Electrophotography. U.S. Patent 4450217, May 22, 1984.

(45) Reynolds, G. A.; Drexhage, K. H. *J. Org. Chem.* **1977**, *42*, 885.

(46) Furukawa, N.; Kobayashi, K.; Sato, S. *J. Organomet. Chem.* **2000**, *611*, 116.

DOI: 10.1021/acs.joc.6b00173
J. Org. Chem. 2016, 81, 3214–3226

(47) Kice, J. L.; Kang, Y. H.; Manek, M. B. *J. Org. Chem.* **1988**, *53*, 2435.
(48) Reich, H. J.; Hoeger, C. A.; Willis, W. W. *J. Am. Chem. Soc.* **1982**, *104*, 2936.
(49) Shimizu, T.; Kobayashi, M.; Kamigata, N. *Bull. Chem. Soc. Jpn.* **1988**, *61*, 3761.
(50) Hayashi, S.; Nakanishi, W.; Furuta, A.; Drabowicz, J.; Sasamori, T.; Tokitoh, N. *New J. Chem.* **2009**, *33*, 196.
(51) Rusakov, Y. Y.; Krivdin, L. B.; Potapov, V. A.; Penzik, M. V.; Amosova, S. V. *Magn. Reson. Chem.* **2011**, *49*, 389.
(52) Kandasamy, K.; Kumar, S.; Singh, H. B.; Wolmershäuser, G. *Organometallics* **2003**, *22*, 5069.
(53) Rusakov, Y. Y.; Krivdin, L. B.; Osterstrom, F. F.; Sauer, S. P. A.; Potapov, V. A.; Amosova, S. V. *Phys. Chem. Chem. Phys.* **2013**, *15*, 13101.
(54) Tripathi, S. K.; Sharma, S.; Singh, H. B.; Butcher, R. J. *Org. Biomol. Chem.* **2011**, *9*, 581.
(55) Yu, S.-C.; Borchert, A.; Kuhn, H.; Ivanov, I. *Chem. - Eur. J.* **2008**, *14*, 7066.
(56) Tripathi, S. K.; Patel, U.; Roy, D.; Sunoj, R. B.; Singh, H. B.; Wolmershäuser, G.; Butcher, R. J. *J. Org. Chem.* **2005**, *70*, 9237.
(57) Mammi, M.; Bardi, R.; Traverso, G.; Bezzi, S. *Nature* **1961**, *192*, 1282.
(58) Hordvik, A.; Sletten, E.; Sletten, J. *Acta Chem. Scand.* **1969**, *23*, 1377.
(59) Cordero, B.; Gomez, V.; Platero-Prats, A. E.; Reves, M.; Echeverria, J.; Cremades, E.; Barragan, F.; Alvarez, S. *Dalton Trans.* **2008**, 2832.
(60) Allen, C.; Boeyens, J. C. A.; Briggs, A. G.; Denner, L.; Markwell, A. J.; Reid, D. H.; Rosea, B. G. *J. Chem. Soc., Chem. Commun.* **1987**, *0*, 967.
(61) Aucott, S. M.; Milton, H. L.; Robertson, S. D.; Slawin, A. M. Z.; Woollins, J. D. *Heteroat. Chem.* **2004**, *15*, 530.
(62) Fuller, A. L.; Knight, F. R.; Slawin, A. M. Z.; Woollins, J. D. *Eur. J. Inorg. Chem.* **2010**, *2010*, 4034.
(63) Bondi, A. *J. Phys. Chem.* **1964**, *68*, 441.
(64) Lamotte, J.; Campsteyn, H.; Dupont, L.; Vermeire, M. *Cryst. Struct. Commun.* **1977**, *6*, 749.
(65) Khatik, G. L.; Kumar, R.; Chakraborti, A. K. *Org. Lett.* **2006**, *8*, 2433.
(66) Frisch, M. J.; Trucks, G. W.; Schlegel, H. B.; Scuseria, G. E.; Robb, M. A.; Cheeseman, J. R.; Scalmani, G.; Barone, V.; Mennucci, B.; Petersson, G. A.; Nakatsuji, H.; Caricato, M.; Li, X.; Hratchian, H. P.; Izmaylov, A. F.; Bloino, J.; Zheng, G.; Sonnenberg, J. L.; Hada, M.; Ehara, M.; Toyota, K.; Fukuda, R.; Hasegawa, J.; Ishida, M.; Nakajima, T.; Honda, Y.; Kitao, O.; Nakai, H.; Vreven, T.; Montgomery, J. A., Jr.; Peralta, J. E.; Ogliaro, F.; Bearpark, M.; Heyd, J. J.; Brothers, E.; Kudin, K. N.; Staroverov, V. N.; Kobayashi, R.; Normand, J.; Raghavachari, K.; Rendell, A.; Burant, J. C.; Iyengar, S. S.; Tomasi, J.; Cossi, M.; Rega, N.; Millam, J. M.; Klene, M.; Knox, J. E.; Cross, J. B.; Bakken, V.; Adamo, C.; Jaramillo, J.; Gomperts, R.; Stratmann, R. E.; Yazyev, O.; Austin, A. J.; Cammi, R.; Pomelli, C.; Ochterski, J. W.; Martin, R. L.; Morokuma, K.; Zakrzewski, V. G.; Voth, G. A.; Salvador, P.; Dannenberg, J. J.; Dapprich, S.; Daniels, A. D.; Farkas, Ö.; Foresman, J. B.; Ortiz, J. V.; Cioslowski, J.; Fox, D. J. *Gaussian 09*; Gaussian, Inc.: Wallingford, CT, 2010
(67) Iwaoka, M.; Komatsu, H.; Katsuda, T.; Tomoda, S. *J. Am. Chem. Soc.* **2004**, *126*, 5309.
(68) Roy, D.; Sunoj, R. B. *J. Phys. Chem. A* **2006**, *110*, 5942.
(69) Sarma, B. K.; Mugesh, G. *ChemPhysChem* **2009**, *10*, 3013.
(70) *Atoms in Molecules: A quantum Theory*; Bader, R. F. W., Ed.; Oxford University Press: New York, 1990.
(71) Iwaoka, M.; Tomoda, S. *J. Org. Chem.* **1995**, *60*, 5299.
(72) Behera, R. N.; Panda, A. *RSC Adv.* **2012**, *2*, 6948.
(73) Roy, D.; Sunoj, R. B. *J. Mol. Struct.: THEOCHEM* **2007**, *809*, 145.
(74) Schleyer, P. v. R.; Maerker, C.; Dransfeld, A.; Jiao, H.; Hommes, N. J. R. v. E. *J. Am. Chem. Soc.* **1996**, *118*, 6317.
(75) Zywietz, T. K.; Jiao, H.; Schleyer, P. v. R.; de Meijere, A. *J. Org. Chem.* **1998**, *63*, 3417.
(76) Perrin, D. D.; Armargo, W. L. F.; Perrin, D. R. *Purification of Laboratory Chemicals*, 4th ed.; Butterworth-Heinemann: Oxford, U.K., 1996.
(77) Thompson, D. P.; Boudjouk, P. *J. Org. Chem.* **1988**, *53*, 2109.
(78) Engman, L.; Persson, J. *J. Organomet. Chem.* **1990**, *388*, 71.
(79) Bader, R. F. W. *Atoms in Molecules: A Quantum Theory*; Oxford University Press: New York, 1990.
(80) Popelier, P. *Atoms in Molecules: An Introduction*; Prentice Hall: Upper Saddle River, NJ, 2000.
(81) Matta, C. F.; Boyd, R. J. *The Quantum Theory of Atoms in Molecules: From Solid State to DNA and Drug Design*; Wiley-VCH: Weinheim, 2007.
(82) Biegler-Konig, F.; Schonbohm, J.; Bayles, D. *J. Comput. Chem.* **2001**, *22*, 545.
(83) Sheldrick, G. M. *SHELXS-97, Program for Crystal Structure Solution*; University of Göttingen: Göttingen, Germany, 1997.
(84) Sheldrick, G. M. *Program for Crystal Structure Solution*; University of Göttingen: Göttingen, Germany, 1997.
(85) *International Tables for X-ray Crystallography*; Kynoch Press: Birmingham, 1974; Vol. *4*.

DOI: 10.1021/acs.joc.6b00173
J. Org. Chem. 2016, 81, 3214−3226